# Unusual mixed valent $Fe^{III}Fe^{II}$ complex ($S_t$ = 3/2) stabilised by a reduced bulky 1,2-diketone

**Geoffrey H. Spikes, Eckhard Bill, Thomas Weyhermüller and Karl Wieghardt***

*Received (in Cambridge, UK) 24th August 2007, Accepted 18th September 2007*
*First published as an Advance Article on the web 4th October 2007*
**DOI: 10.1039/b713062g**

**The reduction of the bulky 1,2-diketone bis(2,6-diisopropylphenyl)glyoxal (1) and $FeBr_2$ with 1.5 equivalents of Na results in a Class 2 mixed valent H.S. $Fe^{II}$ L.S. $Fe^{III}$ complex (2) with two five-coordinate Fe centres which are antiferromagnetically exchange-coupled to give a total spin $S_t$ = 3/2 ground state and an $S_t$ = 5/2 excited state that are separated by about 25 $cm^{-1}$ (for $\Delta_J \approx 5J$)**

Mixed-valent $Fe^{III}Fe^{II}$ complexes are of interest from a fundamental point of view as well as biological mimics. Mixed-valent pairs are present in the active sites of a number of metalloproteins. $Fe^{III}Fe^{II}$ pairs have been implicated in purple acid phosphatase, ribonucleotide reductase, methane monooxygenase and hemerythrin.[1] In enzyme systems the two metal ions usually reside in chemically different environments with differences observed in coordination number, ligand environment and geometry.[2] Most reported model complexes in contrast imply equivalent environments for the two metal ions since symmetrical dinucleating ligands greatly simplify the synthetic problem. In nearly all these enzymes and most of the model complexes which have been synthesised antiferromagnetic coupling and vibronic trapping results in valence localised systems with $S$ = 1/2 ground states.[3] In a few rare examples parallel coupling of electronic spins has resulted in a valence delocalised $S$ = 9/2 ground state.[4]

The bulky 1,2-diketone bis(2,6-diisopropylphenyl)glyoxal **1** was prepared *via* the reaction of CO with the corresponding aryllithium species, using the method reported by Nudelman *et al.*,[5] (Scheme 1) and characterised by X-ray crystallography, NMR spectoscopy and mass spectrometry.† The CO distance at 1.214(2) Å indicates C=O double bonds and the C–C bond of the diketone unit, which lies about an inversion centre, at 1.558(2) Å is typical for a C–C single bond.‡

The addition of **1** in DME at *ca.* 25 °C to 1 equiv. anhydrous $FeBr_2$ and 1.5 equiv. of Na with stirring led over the course of 4 h to a gradual colour change from pale yellow to deep blue. Filtration followed by removal of the solvent *in vacuo* led to the isolation of a blue powder. Subsequent recrystallization from a 90 : 10 mixture of DME–pentane at *ca.* −30 °C led to to the isolation of blue needles of $[Na(DME)_3][Fe^{II}Fe^{III}Br_2(L^{Red})_2(DME)]$ (**2**) (Fig. 1), suitable for single-crystal X-ray diffraction, in moderate yield, (∼40%) where $(L^{Red})^{2-}$ is the $2e^-$ reduced form of the diketone **1**.

The X-ray crystal structure of **2**§ consists of a highly unsymmetric diiron monoanion with a fully separated Na countercation coordinated by three equivalents of DME. Each iron centre is five-coordinate retaining one Br (Fig. 2). The ligand environment around Fe1 approximates a square pyramid with the Br apical and the base consisting of two ligand units bound through all four oxygens O1–O4. The glyoxal carbon-carbon bond lengths at 1.364 and 1.365 Å are consistent with a double (1.32 Å) rather than a single (1.53 Å) bond suggesting the ligands have been doubly reduced to diolate ligands. This is also indicated by long

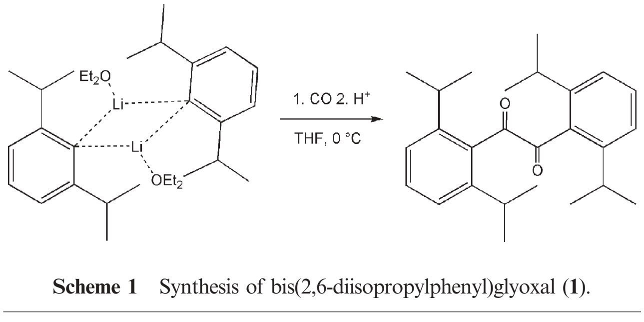

**Scheme 1** Synthesis of bis(2,6-diisopropylphenyl)glyoxal (**1**).

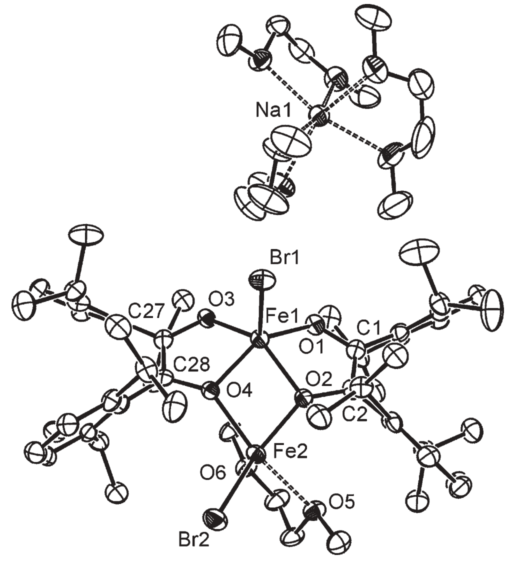

**Fig. 1** Thermal ellipsoid (50%) drawing of **2**, H atoms and solvent molecues are not shown. Selected bond lengths (Å) and angles (°): Fe1–Br1 2.4276(6), Fe1–O1 1.919(3), Fe1–O2 2.043(3), Fe1–O3 1.914(3), Fe1–O4 2.005(3), O1–C1 1.355(5), O2–C2 1.385(5), C1–C2 1.364(6), O3–C27 1.360(5), O4–C28 1.371(5), C27–C28 1.365(5), Fe2–Br2 2.4124(8), Fe2–O2 1.982(3), Fe2–O4 2.116(3), Fe2–O5 2.294(3), Fe2–O6 2.118(3), O1–Fe1–O2 79.86(11), O2–Fe1–O4 77.21(11), O4–Fe1–O3 81.58(11), O3–Fe1–O1 103.10(12), Br1–Fe1–O1 106.82(9), Br1–Fe1–O2 108.16(7), Br1–Fe1–O3 105.71(8), Br1–Fe1–O4 104.32(7), O2–Fe2–O6 104.35(12), O2–Fe2–Br2 144.25(8), O6–Fe2–Br2 110.53(9), O4–Fe2–O5 165.06(11).

---

*MPI für Bioanorganische Chemie, Stiftstrasse 34-36, Mülheim an der Ruhr, 45470, Germany E-mail: wieghardt@mpi-muelheim.mpg.de; Fax: +49 0208-306-3952; Tel: +49 0208-306-3610*

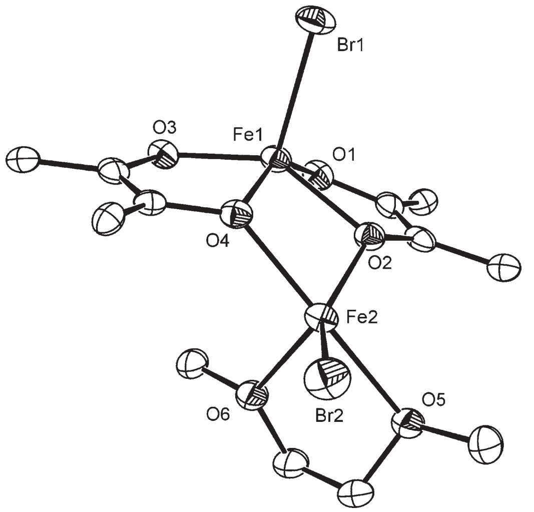

**Fig. 2** Thermal ellipsoid (50%) drawing of close up view of di-iron centre.

carbon–oxygen bond lengths (ranging from 1.355–1.385 Å). The two iron centres are bridged by one oxygen of each ligand, O2 and O4, with the coordination sphere of Fe2 filled by a further equivalent of DME. This defines the long Fe1–Fe2 distance at 3.147 Å. In contrast to Fe1, Fe2 approximates a trigonal bipyramidal geometry with one ligand oxygen, O4, and one of the DME, O5, axial with correspondingly longer bond lengths to Fe2 than O2 and O6. The anion is therefore formulated as a square pyramidal $Fe^{III}$ bridged to a trigonal bipyramidal $Fe^{II}$. The sum of the Fe–Br and the four Fe–O distances is 10.31 Å at Fe1 but 10.92 Å at Fe2 in excellent agreement with the notion that the former is low spin $Fe^{III}$ and the latter high spin $Fe^{II}$.

Compound **2** was further characterized by UV, EPR, SQUID and Mössbauer spectroscopy as well as by elemental analysis. The electronic spectrum of **2** in DME displays a broad intervalence charge transfer band at 702 nm ($\varepsilon \approx 2700\ M^{-1}\ cm^{-1}$). The value of $\Delta\nu_{1/2}$ at 6080 $cm^{-1}$ is close to that calculated from Hush's relationship 5732 $cm^{-1}$ indicative of a Class II mixed-valence system.[6]

The zero field Mössbauer spectrum recorded at 80 K (Fig. 3) shows two rather broad peaks that can be simulated with two quadrupole doublets (I) and (II) in 49 : 51 ratio. Large values for the isomer shift and quadrupole splitting of subspectrum (I), $\delta$ = 1.15 mm $s^{-1}$, $\Delta E_Q$ = 2.29 mm $s^{-1}$, clearly reveal high-spin $Fe^{II}$, whereas a remarkably low isomer shift of only 0.08 mm $s^{-1}$ indicates low-spin $Fe^{III}$ for subspectrum (II). The spectrum is broadened by paramagnetic relaxation, which for the $Fe^{III}$ site is so strong that the quadrupole splitting is not resolved.[7] Due to the excessively large line width of $\omega_{fwhm}$ = 1.58 mm $s^{-1}$ the fitted value for $\Delta E_Q$(II) is probably an under-estimation.

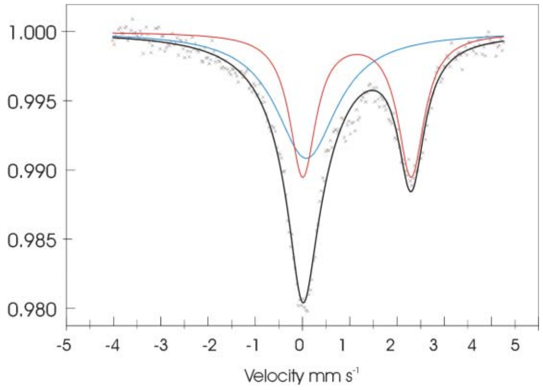

**Fig. 3** Zero-field Mössbauer of solid **2** at 80 K. The red and blue lines are fits with Lorentzian doublets (I) and (II) for high-spin $Fe^{II}$ and low-spin $Fe^{III}$, respectively.

The X-band EPR spectrum of **2** in DME solution at 10 K displays an axial spectrum with a derivative line at $g_\perp \approx 4$ and a negative peak at $g_\parallel \approx 2.2$, that are typical of a spin $S_t = 3/2$ ground state with large zero-field splitting ($D_{3/2} \gg h\nu$). Accordingly, a magnetic susceptibility measurement (Fig. 4) demonstrates a high temperature limit of $\mu_{eff}$ = 5.6 $\mu_B$ consistent with two weakly coupled iron centres, with spin $S_1 = 2$ for $Fe^{II}$ and $S_2 = ½$ for $Fe^{III}$; as one can infer from the relation $\mu_{eff} = [\mu_{eff}{}^2(Fe^{II}) + \mu_{eff}{}^2(Fe^{III})]^{1/2}$ for two un-coupled spins. This yields for the spin-only value $\mu_{eff,s.o.} = g\cdot[S_1(S_1+1) + S_2(S_2+1)]^{1/2}$, which is $g/2\cdot(27)^{1/2}$ or 5.2 $\mu_B$. The higher level of the experimental data was assigned to an increased $g$ value for $Fe^{II}$ of 2.2. The drop of the experimental values of $\mu_{eff}$ below 100 K can be readily assigned to the combined effect of weak anti-ferromagnetic exchange interaction of the two paramagnetic centres with $J = -5.3 \pm 1\ cm^{-1}$, and large zero-field splitting (zfs) of the $Fe^{II}$ high-spin site with $|D| = 10\ cm^{-1}$, as one can see from the simulation shown in Fig. 4.[8]

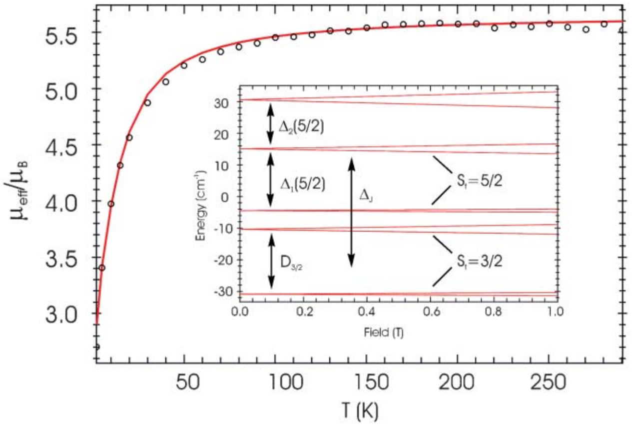

**Fig. 4** Temperature dependence of the magnetic moment, $\mu_{eff}$, of solid **2**. The solid (red) line represents a spin Hamiltonian simulation based on $\hat{H} = -2J\,\hat{\vec{S}}_1\cdot\hat{\vec{S}}_2 + g\beta\left(\hat{\vec{S}}_1 + \hat{\vec{S}}\right)\cdot\vec{B} + D\left[\hat{S}_{1,z}^2 - 2\right]$ with the parameters reported in the text. The inset shows the calculated energy level scheme of the system for fields applied in $z$-direction.

Very little is known about the transition metal coordination chemistry of acyclic 1,2-diketones or their one- and two-electron-reduced forms. To date all reported 1,2 diketone complexes contain the ligand in its two-electron-reduced diolate form with an early transition metal. All were isolated in the course of studies looking at the reductive coupling of aldehydes. As well as 1 : 1 adducts with group 4 metallocenes,[9] complexes with tungsten[10] and chromium[11] are also known. Dimeric tungsten compounds of general formula $W_2(OR)_6(O_2C_2R'_2)_2$ (R = $^tBu$, R′ = Ph and R = $^iPr$, R′ = Me, $p$-Tol or Ph) were synthesised by direct reaction of $W_2(OR)_6$ with the diketone and demonstrated bridging alkoxides and a W–W single bond consistent with ligand reduction and oxidation of the metal centre from $(W{\equiv}W)^{6+}$ to $(W{-}W)^{10+}$.[10] $Tp^{iPr2}CrO_2C_2Ph_2$ ($Tp^{iPr2}$ = hydrotris(3,5-diisopropylpyrazolyl)borato) a 1 : 1 chromium diolate adduct was formed by the reductive coupling of benzaldehyde by $Tp^{iPr2}CrCl{\cdot}py$.[11] In our system two diketone ligands have been fully reduced to their diolate form corresponding to the oxidation of three equivalents of Na metal and one $Fe^{II}$ centre to $Fe^{III}$. Cyclic voltammetry shows only one reversible feature at −1.62 *vs.* $Fc/Fc^+$ which we assign to the reduction of $Fe^{III}$ to $Fe^{II}$. It appears that any oxidation of **2** leads to decomposition of the dimer. Unlike all previously reported mixed valent iron dimers the high spin state of the $Fe^{II}$ antiferromagnetically coupled to the low spin state of the $Fe^{III}$ leads to a ground state of $S_t = 3/2$.

G.H.S. would like to thank the Alexander V. Humboldt Foundation for the award of a Fellowship.

## Notes and references

† All manipulations except ligand workup were conducted under strict exclusion of air and moisture in an atmosphere of dry argon or *in vacuo* using Schlenk line and glovebox techniques. $Li_2(Et_2O)_2(C_6H_3\text{-}2,6\text{-}Pr^i_2)_2$ was prepared by modification of the procedure for $Li_2(Et_2O)_2(C_6H_2\text{-}2,4,6\text{-}Pr^i_3)_2$.[12] ESI mass spectra were obtained on a Finnigan MAT 95 spectrometer. Elemental analyses were done by the H. Kolbe Mikroanalytisches Laboratorium in Mülheim an der Ruhr, Germany. Variable temperature magnetic susceptibilities were measured on a Quantum Design SQUID magnetometer in the range 2–300 K at an applied external field of 1000 G. Data points were corrected for intrinsic diamagnetism of the sample, the sample holder, and also for temperature-independent paramagnetism. The magnetic data were simulated by using our own spin Hamiltonian program julX for exchange-coupled systems (written by E.B.). X-Band EPR spectra were recorded at 10 K on a Bruker ESP 300E spectrometer equipped with a helium-flow cryostat (Oxford Instruments ESR 910). Mössbauer spectra were recorded on a spectrometer with alternating constant-acceleration. The minimum experimental line width was 0.24 mm $s^{-1}$. The sample temperature was maintained constant by an Oxford Instruments Variox cryostat. Isomer shifts (δ) are referenced against iron metal at 300 K.

Bis(2,6-diisopropylphenyl)glyoxal, **1**: A solution of $Li_2(Et_2O)_2(C_6H_3\text{-}2,6\text{-}Pr^i_2)_2$ (5 g, 12.2 mmol) in THF (20 mL) was cooled to 0 °C. CO was bubbled through the solution resulting in a colour change from pale yellow to dark red. The solution was allowed to warm to room temperature and exposed to air. The solution was washed with quenched with water (20 mL) and extracted with $Et_2O$ (50 mL). Removal of the solvent in vacuo resulted in a pale yellow residue. This was extracted with hexane and recrystallised to give **1** as pale yellow crystals (Yield 1.5 g, 4.0 mmol, 32%). $^1H$ NMR ($CDCl_3$, 300.08 MHz): δ(ppm) 1.17 (d, 24H, $J$ = 6.9 Hz, $CHMe_2$), 2,61 (sept,. 4H, $J$ = 6.6 Hz, $CHMe_2$), 7.20 (d, 4H, Ar–H), 7.38 (t, 2H, Ar–H). $^{13}C$ NMR ($C_6D_6$, 100.52 MHz): δ(ppm) 22.6 ($CHMe_2$), 32.1 ($CHMe_2$), 123.1, 130.3, 134.5, 145.9 (unsaturated carbon) 199.5 (ArCO),. Mass spectrum (ESI): $m/z$ = 189, ($COC_6H_3\text{-}2,6\text{-}Pr^i_2$, 100%), $m/z$ = 161 ($C_6H_3\text{-}2,6\text{-}Pr^i_2$, 32%).

$Fe^{II}Fe^{III}$, **2**: A solution of **1** (100 mg, 0.26 mmol) in DME (8 mL) was added with stirring to $FeBr_2$ (56 mg, 0.26 mmol) and Na (9.2 mg, 0.4 mmol). The pale yellow solution turned deep blue over 4 h. Removal of the solvent *in vacuo* resulted in a deep blue residue which was extracted in 90 : 10 pentane–DME (3 mL) and filtered. Storage at −30 °C yielded **2** as blue crystals in moderate yield (77 mg, 0.05 mmol, 41%). UV-Vis (*DME*): 702 nm (ε = 2700). Elemental Analysis (**2** + 2NaBr) Expected C 51.2% H 6.95% Found C 51.5% H 6.80%)

Crystal data for **1** and **2** at 100(2) K with $MoK_\alpha$ ($\lambda = 0.71073$ Å). **1**: $M$ = 378.53, orthorhombic, space group *Pbca*, $a$ = 9.6205(3) Å, $b$ = 13.8569(5) Å, $c$ = 16.7988(6) Å, $\alpha = \beta = \gamma = 90°$, $Z$ = 4, $R1$ = 0.0426 for 2031 ($I > 2\sigma(I)$) reflections, $wR2$ = 0.1065 (all data); **2**: $M$ = 1448.13, orthorhombic, space group *Fdd2* No. 43, $a$ = 38.156(2) Å, $b$ = 50.415(3) Å, $c$ = 15.8144(8) Å, $\alpha = \beta = \gamma = 90°$, $Z$ = 16, $R1$ = 0.0494 for 11475 ($I > 2\sigma(I)$) reflections, $wR2$ = 0.0990 (all data).

‡ CCDC 658636. For crystallographic data in CIF or other electronic format see DOI: 10.1039/b713062g

§ CCDC 658637. For crystallographic data in CIF or other electronic format see DOI: 10.1039/b713062g

1 (*a*) D. M. Kurtz, *Chem. Rev.*, 1990, **90**, 585; (*b*) A. Neves, M. A. de Brito, I. Vencato, V. Drago, K. Griesar and W. Haase, *Inorg. Chem.*, 1996, **35**, 2360; (*c*) B. J. Wallar and J. D. Lipscomb, *Chem. Rev.*, 1996, **96**, 2625; (*d*) E. I. Solomon, T. C. Brunold, M. I. Davis, J. N. Kemsley, S.-K. Lee, N. Lehnert, F. Neese, A. J. Skulan, Y.-S. Yang and J. Zhou, *Chem. Rev.*, 2000, **100**, 235; (*e*) M. Merkx, D. Kopp, M. H. Sazinsky, J. L. Blazyk, J. Muller and S. J. Lippard, *Angew. Chem., Int. Ed.*, 2001, **40**, 2782.

2 C. Belle and J.-L. Pierre, *Eur. J. Inorg. Chem.*, 2003, 4137.

3 (*a*) G. Blondin and J. J. Girerd, *Chem. Rev.*, 1990, **90**, 1359; (*b*) E. Bernard, W. Moneta, J. Laugier, S. Chardon-Noblat, A. Deronzier, J.-P. Tuchagues and J.-M. Latour, *Angew. Chem., Int. Ed. Engl.*, 1994, **33**, 887; (*c*) J. D. Cohen, S. Payne, K. S. Hagen and J. Sanders-Loehr, *J. Am. Chem. Soc.*, 1997, **119**, 2960; (*d*) E. I. Solomon, D. W. Randall and T. Glaser, *Coord. Chem. Rev.*, 2000, **200**, 595; (*e*) S. Albedyhl, M. T. Averbuch-Pouchot, C. Belle, B. Krebs, J.-L. Pierre, E. Saint-Aman and S. Torelli, *Eur. J. Inorg. Chem.*, 2001, 1457.

4 (*a*) S. Drüeke, P. Chaudhuri, K. Pohl, K. Wieghardt, X.-Q. Ding, E. Bill, A. Sawaryn, A. X. Trautwein, H. Winkler and S. J. Gurman, *J. Chem. Soc., Chem. Commun.*, 1989, 59; (*b*) D. R. Gamelin, E. L. Bominaar, M. L. Kirk, K. Wieghardt and E. I. Solomon, *J. Am. Chem. Soc.*, 1996, **118**, 8085; (*c*) S. K. Dutta, J. Ensling, R. Werner, U. Flörke, W. Haase, P. Gütlich and K. Nag, *Angew. Chem., Int. Ed. Engl.*, 1997, **36**, 152; (*d*) J. R. Hagadorn, L. Que, Jr., W. B. Tolman, I. Prisecaru and E. Münck, *J. Am. Chem. Soc.*, 1999, **121**, 9760; (*e*) D. Lee, C. Krebs, B. H. Huynh, M. P. Hendrich and S. J. Lippard, *J. Am. Chem. Soc.*, 2000, **122**, 5000; (*f*) A. Stubna, D.-H. Jo, M. Costas, W. W. Brenessel, H. Andres, E. L. Bominaar, E. Münck and L. Que, Jr., *Inorg. Chem.*, 2004, **43**, 3067.

5 N. S. Nudelman and P. Outumuro, *J. Org. Chem.*, 1982, **47**, 4347.

6 (*a*) N. S. Hush, *Prog. Inorg. Chem.*, 1967, **8**, 391; (*b*) C. Creuz, *Prog. Inorg. Chem.*, 1983, **30**, 1.

7 The broadening is apparently stronger for $Fe^{III}$ ($S_2 = 1/2$) than for $Fe^{II}$ ($S_1 = 2$), although the local spins are coupled by sizable exchange interaction ($J = -5.3$ $cm^{-1}$), so that the paramagnetic relaxation rate should be the same for both sites. We assign this effect to the larger magnetic anisotropy expected for the ferric low-spin site, due to strong spin–orbit coupling.

8 The parameters render the sextet excited state manifold at about 25 $cm^{-1}$ above the quartet ground state, according to an exchange splitting $\Delta_J$ of about $5|J|$, as it would be expected for the limiting case of vanishing zfs. However, the manifolds are actually mixed by the large zfs coming from $Fe^{II}$, as can be seen from the energy level scheme shown in the inset of Fig. 4. The ratio of the effective zfs $\Delta_1(5/2)$ and $\Delta_2(5/2)$ of the three Kramers doublets of the excited sextet apparently deviates significantly from the expected scheme $2D_{5/2}/4D_{5/2}$.

9 (*a*) P. Hofmann, M. Frede, P. Stauffert, W. Lasser and U. Thewalt, *Angew. Chem., Int. Ed. Engl.*, 1985, **24**, 712; (*b*) G. Erker, P. Czisch, R. Schlund, K. Angermund and C. Krüger, *Angew. Chem., Int. Ed. Engl.*, 1986, **25**, 364; (*c*) L.-C. Song, P.-C. Liu, C. Han and Q.-M. Hu, *J. Organomet. Chem.*, 2002, **648**, 119.

10 M. H. Chisholm, J. C. Huffman and A. L. Ratermann, *Inorg. Chem.*, 1983, **22**, 4100.

11 K.-I. Sugawara, S. Hikichi and M. Akita, *J. Chem. Soc., Dalton Trans.*, 2002, 4514.

12 R. A. Bartlett, H. V. R. Dias and P. P. Power, *J. Organomet. Chem.*, 1988, **341**, 1.